



This open access document is published as a preprint in the Beilstein Archives with doi: 10.3762/bxiv.2019.21.v1 and is considered to be an early communication for feedback before peer review. Before citing this document, please check if a final, peer-reviewed version has been published in the Beilstein Journal of Nanotechnology.

This document is not formatted, has not undergone copyediting or typesetting, and may contain errors, unsubstantiated scientific claims or preliminary data.

Preprint Title Self-assembly and cell imaging behaviors of Tripeptide-naphthalenediimide and interactions with carbon nano-materials

Authors Zhou Xiao, Yang Wang, Jie zhang and Zhiyuan Hu

Article Type Full Research Paper

Supporting Information File 1 supporting information.pdf; 1.8 MB

ORCID® iDs Zhiyuan Hu - <https://orcid.org/0000-0002-7901-686X>

Self-assembly and cell imaging behaviors of Tripeptide-naphthalenediimide and interactions with carbon nanomaterials

Zhou Xiao^a, Yang Wang^a, Jie Zhang^a, Zhiyuan Hu^{a*}

^aCollege of Science, China University of Petroleum (Beijing), Beijing 102249, China

* Corresponding author.

E-mail address: zh209@cup.edu.cn (Z. Hu)

Abstract

Compared with other self-assembling molecule, peptide, especially unprotected peptide have better biocompatibility and are more acceptable for food science, cosmetics and biopharmaceuticals. However, the regulation of the microstructure formed by peptide self-assembled supramolecular remains a major problem. Herein we have designed three amphiphilic supramolecular that can self-assemble to form specific structures. The amphiphilic supramolecular use 1,4,5,8-naphthalenetetracarboxylic anhydride as the self-assembling framework to form some specific nanostructure by the regulation of the tripeptide molecule attached to both ends of the naphthalene diimide molecules. As designed, we have observed nanostructures such as spheres, squares, and needles formed under acidic or basic condition by electron microscopy images. And we attached the molecule to the carbon six-membered ring structure of carbon nanotubes and graphene, which provides a method for improving the dispersibility of carbon nanotubes and graphene. The peptide-based molecular designs enforce intimate π - π communication and hydrogen bonding within the aggregates after self-assembly, making these nanostructures attractive for optical or electronic applications in biological environments.

Keywords

Self-assembly, naphthalene diimide, tripeptide, carbon materials, cell fluorescence

Introduction

As protein self-assembly is widespread in nature, Materials science and biomedicine show great interest in the molecular self-assembly of oligopeptides since the first example of short self-assembled peptide [1,2]. Twenty kinds of essential amino acids can synthesize tens of thousands of oligopeptides with different structures and functions. This facilitates the selection of structures and the optimization of the condition for self-assembly of oligopeptides. In addition, since the polypeptide is a biologically active substance involved in various cellular functions in the living body, it also has good biocompatibility and controllable degradation compared to most organic polymers. For those reasons, molecular self-assembly of oligopeptides holds much promise for a range of broader applications in biomedicine [3-6], biochemical materials [7-10] compared with other self-assembled systems. In the early years there have been many reports of long peptide chain [11-13]. But most of the reported sequences are based on known peptide sequences that have been discovered unintentionally or mapped to biological systems [14-16]. Compared to long peptide chains, the synthesis of short peptide chains is simpler and easier to study the self-assembly rules. Self-assembly of short peptides has been previously reported [17-20], but the self-assembly rules based on unprotected tripeptides are still ambiguous and only a small fraction of the available sequence is explored. In order to solve this problem and find the general rule of self-assembly of short peptides, some scholars²¹ have completely and fairly simulated the all possible amino acid combinations in the tripeptide ($20^3=8000$ different sequences) to predict the aggregation tendency. They derived the amino acid arrangement of tri-peptides that are easy to self-assemble: All tri-peptides that are susceptible to aggregation comprise a pair of adjacent aromatic amino acids and at least one phenylpropanoid residue. In addition, a positively charged

or hydrogen bondable amino acid is usually in the first position. This has helped tremendously in designing short peptide molecules that can be used for self-assembly.

In the molecular self-assembly design process based on amino acid or short peptide sequences, hydrophobic groups (such as aliphatic chain hydrophobic groups) are usually added to the structure to promote self-assembly to form a three-dimensional structure [22]. Another important way is to add aromatic hydrophobic functional groups (such as naphthalene-bisimide [23-26], Fmoc [27,28], azobenzene [29], 4,4'-bipyridyl [30] and pyrene derivatives [31,32]) to the amino-terminus of amino acids or polypeptide chains. In this study, we used 1,4,5,8-naphthalenediimide (NDI) as a hydrophobic group to form amphiphilic polypeptide self-assembling molecules.

NDI is an arylene-based chromophore and is the most promising n-type semiconductor for electronic devices based on organic materials [33,34]. Due to its high electron affinity and good carrier mobility, it is an excellent electron acceptor. It also has good electrochemical properties, high light stability and a fluorescence quantum yield of approximately 100%. NDI and its derivatives are relatively easily-functionalized materials [35,36] that have strong absorption and fluorescence emission in the visible and near-IR wavelengths. This makes NDI-based derivatives attractive candidates as building blocks for optical imaging probes. At the same time, the DNA-embedding properties, antibacterial and anti-tumor properties of NDI molecules make them promising for future biomedical applications [37]. Compared to other aromatic imides, NDI and its derivatives have better process-ability owing to their enhanced solubility. T. Govindaraju et al [38] pointed out that the main challenge in organizing aromatic moieties lies in controlling and optimizing the relatively strong π - π interactions by adjusting the substituents. Combining NDI and long-chain alkyl, alkoxy or phenyl substituent is the most common method [39,40]. But most

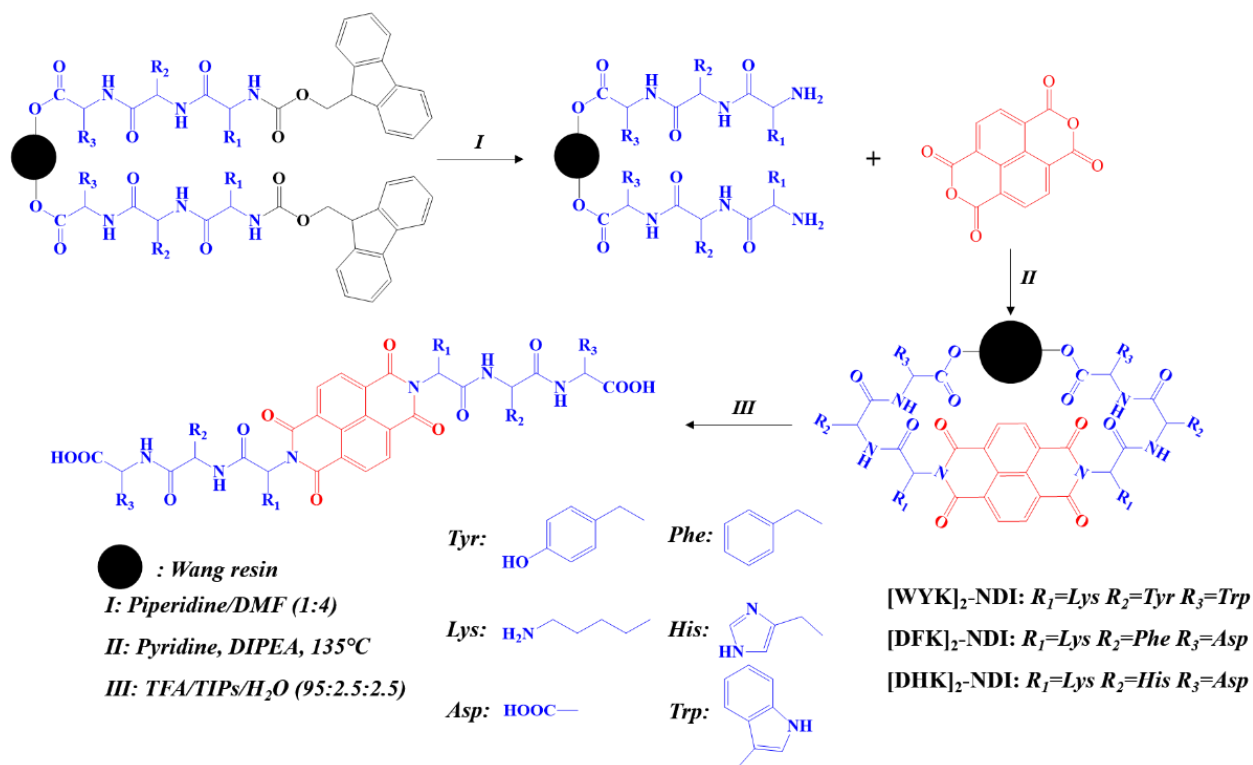
of these groups only provide a single intermolecular force. For example, the alkyl group provides hydrophobic effect, the phenyl group provides π stacking action, and the alkoxy group provides a hydrogen bonding action. Since amino acids and short peptide molecules can simultaneously provide multiple intermolecular forces to promote and regulate self-assembly, scholars have gradually shifted their attention to amino acid and peptide molecules.

Based on the aggregation tendency of the tri-peptide sequences mentioned above, we chose three tri-peptide sequences with high aggregation tendency to research the self-assembly of the three sequences. In order to enhance the possibility of self-assembly, the NDI was used as an aromatic hydrophobic functional group to conjugate with tri-peptide to form an amphiphilic molecule. On the one hand, NDI provides a strong π - π stacking effect for self-assembly and provides a skeleton for the formation of nanostructures of amphiphilic molecules. On the other hand, the introduction of amino acids can control and optimize the relatively strong π - π interaction of NDI while providing additional and not a single force (such as hydrophilicity, hydrophobicity, directionality and hydrogen bonding) for the nanostructure composition of NDI. Compared to some previously reported self-assembled peptide derivatives and NDI derivatives, the molecules we synthesized were completely new molecules obtained by design, rather than products obtained by accidental discovery or bio-mapping. This means that we have taken another step toward the goal of being able to design our own self-assembled structures with specific functional structures. Just as designed, our synthesized molecules can self-assemble with NDI as a skeleton to form different nano-microstructures (such as squares, spheres and needle shape) under acidic or basic condition. The π - π interaction is the main driving force, and the force of hydrogen bond and aromaticity provided by amino acids and its branches is the regulating force. Due to the fluorescent properties of NDI and the biocompatibility of unprotected peptide chains,

they have potential applications in biological sciences such as fluorescent probes and cell fluorescence imaging [41]. The polyphenylene ring structure of NDI also enables us to successfully attach NDI amphiphilic molecules to carbonaceous materials such as carbon nanotubes and graphene through a combination with a carbon six-membered ring. The amphiphilic nature of the molecule can effectively improve the dispersibility of the carbon material to facilitate its further application. It also provides a method for binding bioorganic molecules to carbon materials without changing the inherent structure of the carbon materials.

Results and Discussion

All peptides were synthesized using standard solid phase 9-fluorenylmethoxycarbonyl (Fmoc) chemistry on a Wang resin preloaded with the Fmoc protected leading amino acid. The coupling reaction of NDI and the peptide chain was carried out by refluxing in pyridine for 10 hours. To ensure that the peptide in the reaction is in excess so that each NDI molecule is attached to the peptide chain on both sides, we use a two-stage coupling method. That is, 0.6 equivalents of NDI and pyridine were first added, and after 10 hours, the remaining 0.4 equivalents of NDI and pyridine were added to complete the reaction. After 10 more hours, the resin was rinsed and subjected to a “blank” reflux cycle in pyridine to drive maximal imide bond formation. Of course, it is necessary to add diisopropylethylamine in the coupling reaction. The final product was excised from the resin using a resection solution of trifluoroacetic acid. The final powdered product was obtained by precipitation, centrifugation, precipitation, followed by dissolution with a suitable buffer and lyophilization.



Scheme 1. Synthesis of [WYK]₂-NDI, [DFK]₂-NDI and [DHK]₂-NDI.

All three compounds were lyophilized to a powder with different colours. Among them, [WYK]₂-NDI is a light-red powder with a yield of 28.43%. [DFK]₂-NDI is a gray-white powder with a yield of 34.32%. [DHK]₂-NDI is a black-brown powder with a yield of 30.13%. Detailed experimental details and hydrogen spectrum data are in the **supporting information**. All products were stored in a -4 °C refrigerator and stored for long periods in a -20 °C refrigerator. They all have good solubility in neutral, acidic and basic solution. We completely disperse the samples by shaking and sonicating and characterize them by UV, circular dichroism, fluorescence emission, etc.

Uv-Vis @ CD

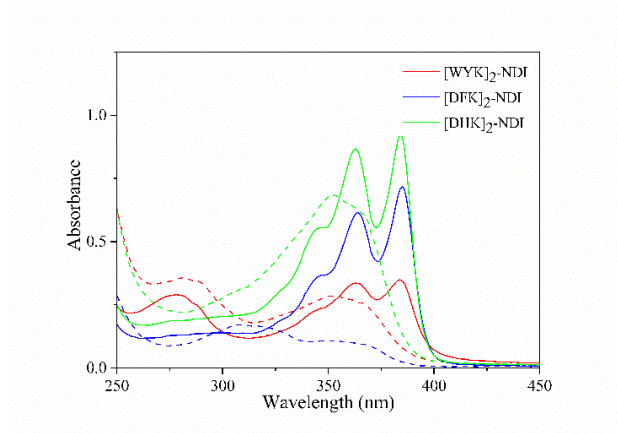


Figure 1. Ultraviolet absorption spectrum of the [WYK]₂-NDI, [DFK]₂-NDI, [DHK]₂-NDI (0.05 wt% in water, solid line: acidic, dotted line: basic, acid: 10 μ L 1 M HCl into 3 mL, basic: 10 μ L 1 M NaOH into 3 mL).

Aqueous solution has the strongest polarity compared to the organic solvent, which promotes the stacking of the aromatic groups of the NDI. As shown in **Figure 1**, the UV absorption spectrum of [WYK]₂-NDI, [DFK]₂-NDI, [DHK]₂-NDI under acidic condition has a strong absorption peak between 330 and 390 nm. Compared to the standard UV absorption peak (340 nm, 358 nm, 378 nm) of the reported NDI amino acid derivative in acetonitrile solution, the UV absorption peaks of [WYK]₂-NDI, [DHK]₂-NDI (347 nm, 363 nm, 384 nm) and [DFK]₂-NDI (347 nm, 364 nm, 385 nm) have a bathochromic shift of about 6 nm. This means that *J*-type aggregation occurs in the NDI in the aqueous solution compared to the NDI in the acetonitrile solution [42,43]. Compared to [DFK]₂-NDI and [DHK]₂-NDI, the absorption intensity of [WYK]₂-NDI is relatively lower, presumably due to the difference in peptide chains, resulting in different morphology and aggregation of aggregates formed. [WYK]₂-NDI may form aggregates with a higher degree of aggregation under acidic condition, and relatively less surface area. In addition to the three characteristic peaks between 330-390 nm, [WYK]₂-NDI also has an absorption peak at 280 nm. It is due to the presence of a tryptophan residue and a tyrosine residue in the

molecule, and a conjugated double bond exists inside the molecule. The UV absorption peak at 280 nm is also an identification condition commonly used to identify proteins.

In the acidic solution, a low pH causes the molecule to absorb protons to cause the protonation effect. However, in the basic solution deprotonates the carboxyl group of the peptide chain due to the addition of sodium hydroxide. This results in different aggregation of molecules. It can be clearly seen that the ultraviolet absorption peak of [WYK]₂-NDI and [DHK]₂-NDI are attenuated to only one broad absorption peak at 354 nm, and a significant blue shift occurs. It can be speculated that the absorption peak at 354 nm is derived from the absorption peak at 363 nm. [DFK]₂-NDI also has a broad absorption peak at 354 nm and a significant blue shift. However, unlike [WYK]₂-NDI and [DHK]₂-NDI, the intensity of the absorption peak is greatly reduced. This means that compound [DFK]₂-NDI is more highly aggregated under basic condition. In addition, there is an extra wide peak at 317 nm, which is not seen in [WYK]₂-NDI and [DHK]₂-NDI. NDI is deprotonated to become an anion due to the presence of sodium hydroxide under basic solution. The electrostatic repulsion between the anions would hinder aggregation if other conditions are ignored. However, we can see from the UV absorption spectrum that the degree of aggregation in the basic solution is higher. We deduce that the Na⁺-mediated interaction with the anion of NDI can reduce electrostatic repulsion. That is, *H*-type aggregation occurs in NDI under basic condition.

The *H*-type aggregation is a face-to-face parallel stack, that is, the molecules that are adjacent to each other in the direction perpendicular to the stacking surface can overlap. And the *J*-type aggregation is a staggered parallel stack. That is, adjacent molecules need to move in the vertical direction of the stacking surface and then move in parallel to overlap. *H*-type aggregates have a higher ability than *J*-type aggregates. However, in very polar aqueous solutions, hydrophobic

NDI groups will gather together as much as possible to reduce the area of contact with water molecules. Thus in a hydrophobic solution, *H*-type aggregation, whose aggregation type is a face-to-face stack, is more likely to form larger volumes of aggregates.

On the other hand, the amount of charge carried by the tripeptide molecule in the acid-base solution will be different. Studies [44,45] have shown that the difference in charge carried by peptide molecules can lead to different self-assembly. They alter the charge of the peptide molecule by amidating the N-terminus or acetylating the C-terminus. The results show that neutral or negative charges favor self-assembly, while positive charges are not conducive to self-assembly. The three samples were all positively charged under the acidic condition of the experiment and negatively charged under the basic condition. It is presumed that the aggregates formed in the acidic solution have smaller size than the aggregates formed in the basic solution.

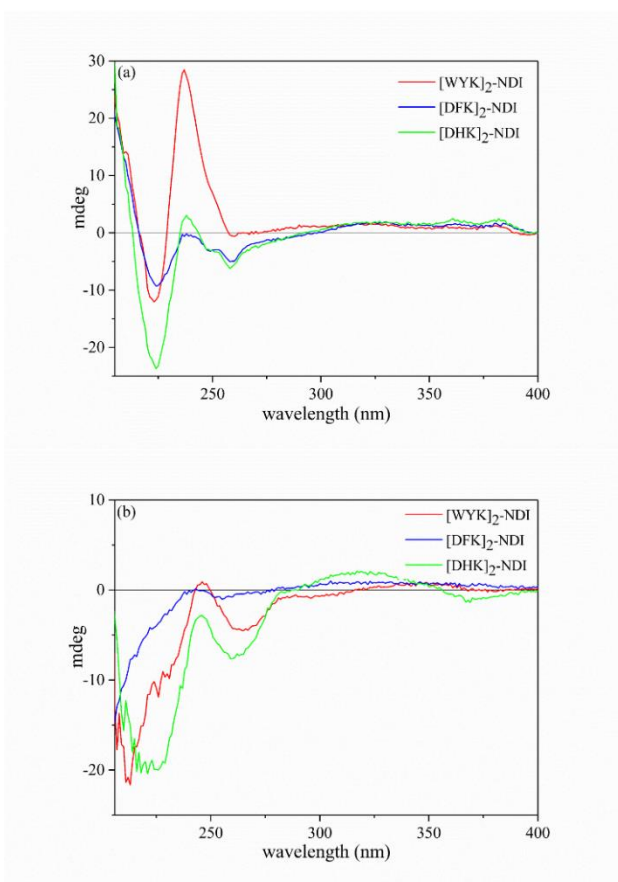


Figure 2. Circular dichroism of the [WYK]₂-NDI, [DFK]₂-NDI, [DHK]₂-NDI under (a) acidic condition (0.5 wt% in water, 10 μ L 1 M HCl into 3 mL) and (b) basic condition (0.5 wt% in water, 10 μ L 1 M NaOH into 3 mL).

The circular dichroic image of all samples is shown in **Figure 2**. In the acidic solution, all three samples showed a pronounced Cotton effect at 223 nm. The negative band at 223 nm is attributed to $n-\pi^*$ transitions of the imide chromophore. Compared to [WYK]₂-NDI and [DFK]₂-NDI, the band intensity of [DHK]₂-NDI is higher. This may be due to the influence of aromatic chromophores in the peptide chain. Conversely, [WYK]₂-NDI has a strong positive band at 238 nm, and [DFK]₂-NDI does not form a positive band here. Surprisingly, [DFK]₂-NDI and [DHK]₂-NDI have similar negative cotton effects at 258 nm, and the intensity and shoulder of the peak are almost the same. The difference is that [WYK]₂-NDI has only a weak negative

cotton effect at 258 nm. This is somewhat similar to the results of the UV absorption spectrum. That is, the key characteristic peaks of [DFK]₂-NDI and [DHK]₂-NDI are somewhat different from [WYK]₂-NDI. It is inferred that the microscopic morphology of [DFK]₂-NDI and [DHK]₂-NDI self-assembly are different from that of [WYK]₂-NDI. The CD spectrum at the free NDI absorbance (330-400 nm) was assigned to interactions between the NDI couplets of sequential interacting NDI chromophores. The three samples have only a weak cotton effect between 350 nm and 400 nm, which is due to the change in the relative position of these parts, resulting in changes in the CD fingerprint of the supramolecular assembly. [WYK]₂-NDI and [DHK]₂-NDI have obvious positive exciton coupled images (from long wave to short wavelength direction) that change from positive cotton effect to negative cotton effect. The exciton coupling effect indicates that the molecules form a helical chiral aggregate. [DFK]₂-NDI has only a few negative cotton effects, but does not form a positive cotton effect, meaning that there is no aggregate of spirals. We speculate that due to the presence of phenylalanine residues, a stronger π stacking effect is provided for the polypeptide chain. This makes the aggregation of the peptide chain more similar to stacking rather than spiral.

In basic solution, [DFK]₂-NDI shows a big difference. There is almost no cotton effect between 205-400 nm (the interval less than 205 nm is not reliable due to equipment accuracy). Perhaps the disordered stacking of molecules in solution leads to the disappearance of the cotton effect. The negative peak of [WYK]₂-NDI at 223 nm is blue-shifted, and the peak of [DHK]₂-NDI at 223 nm is broadened. In addition, [DHK]₂-NDI has a broad negative peak at 259 nm and [WYK]₂-NDI has a broad peak at 265 nm. In the area after 300 nm, [WYK]₂-NDI and [DFK]₂-NDI have almost no cotton effect. The difference is that [DHK]₂-NDI has a new positive cotton effect between 300-350 nm and a negative cotton effect between 350-400 nm.

Morphological Studies

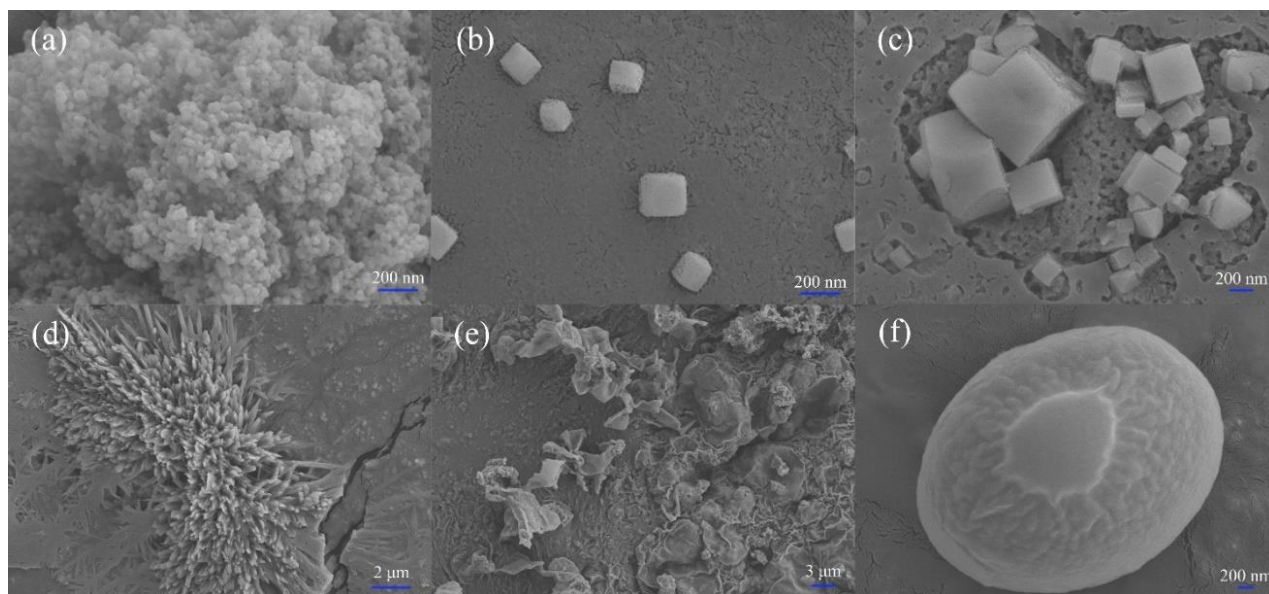
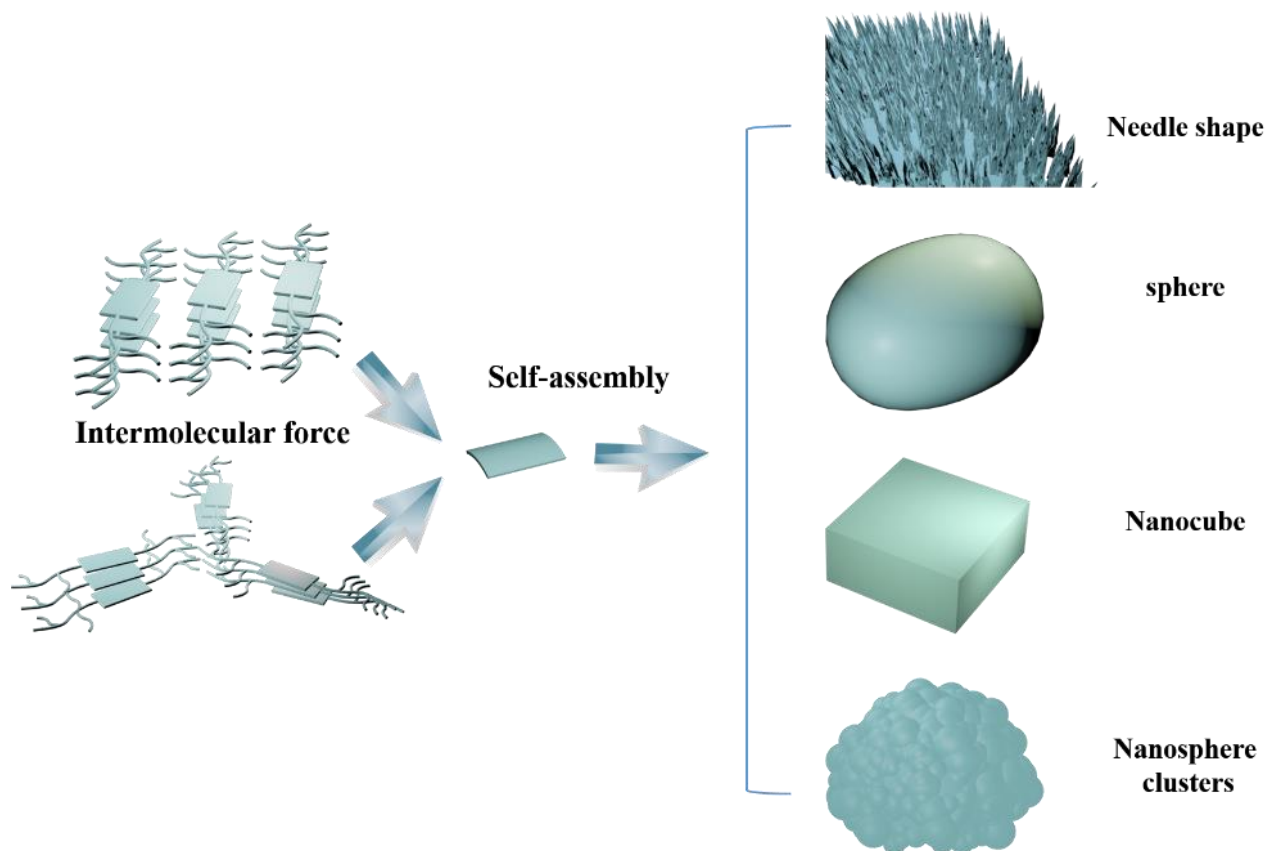


Figure 3. SEM of [WYK]₂-NDI, [DFK]₂-NDI, [DHK]₂-NDI in acid solution (a, b, c) and basic solution (d, e, f) (0.05 wt% in water, acid: 10 μL 1 M HCl into 3 mL, basic: 10 μL 1 M NaOH into 3 mL).



Scheme 2. The schematic diagram of possible microscopic nano-self-assembly of [tripeptide]₂-NDI molecules in acid or basic solutions.

The solution of samples were lyophilized and the topographical feature is shown in **Figure 3** by scanning electron microscopy. [WYK]₂-NDI forms nanosphere clusters about 10 nm in diameter in acidic solution and has a high degree of aggregation. [DFK]₂-NDI and [DHK]₂-NDI form cubical aggregate. But the difference is that the size of cube formed by [DFK]₂-NDI is about 200 nm and the size of cube formed by [DHK]₂-NDI ranges from 200 nm to 500 nm. The combined action of hydrogen bonding, solvophobic force and aromatic stacking shape of the molecular organization and the final morphology. It is difficult to understand the specific interactions between each force and the specific mode of action of each molecule's micromorphology. However, as previously stated, the introduction of the peptide chain regulates the stronger π - π

stacking of NDI, thereby regulating self-assembly to form ordered aggregates. It can be inferred that for [DFK]₂-NDI and [DHK]₂-NDI, the hydrogen bond provided by the aspartic acid residue at the end of the molecule is critical for the formation of the cube. Surprisingly, [WYK]₂-NDI formed a wonderful needle shape under basic condition. Similarly, [DFK]₂-NDI and [DHK]₂-NDI have undergone tremendous changes due to the deprotonated morphology of sodium hydroxide. [DHK]₂-NDI forms a single sphere with a diameter of about 4 μm. All of the above molecules form a certain regular aggregate. However, [DFK]₂-NDI formed an irregularly curled aggregate after deprotonation. It is also seen in the ultraviolet spectrum that the ultraviolet absorption peak of [DFK]₂-NDI under basic condition becomes very wide and low, and the degree of aggregation is high. In addition, no significant cotton effect in the circular dichroism also means random curling.

Fabrication of [Tripeptide]₂-NDI @Graphene and Tripeptide-NDI@Carbon Nanotubes Composites

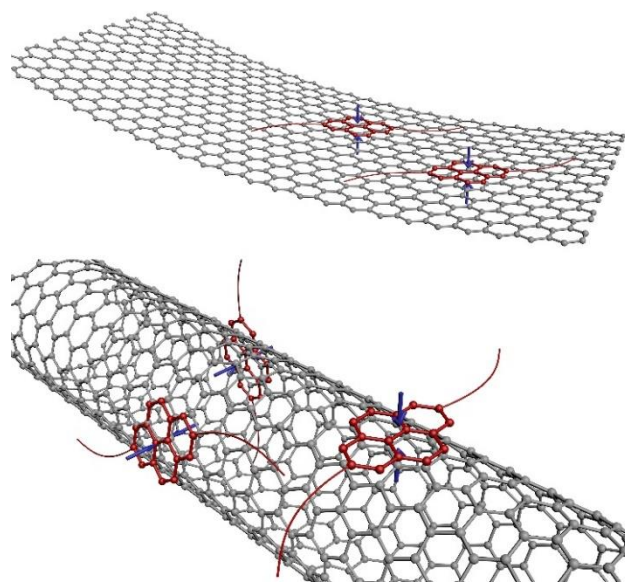


Figure 4. [Tripeptide]₂-NDI molecules are combined with carbon nanotubes and graphene

through a carbon six-membered ring.

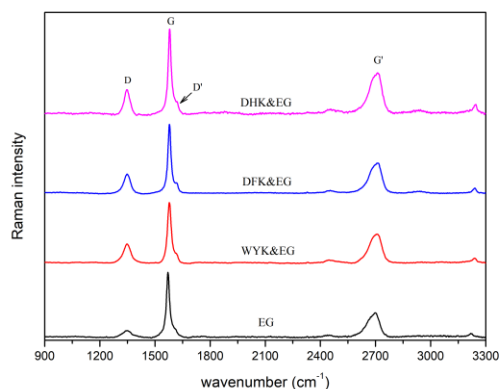


Figure 5. Spectroscopy of pure EG and NDI-functionalized EG. Showing D and G bands for pure EG and [WYK]₂-NDI, [DFK]₂-NDI, [DHK]₂-NDI (CHCl₃: EtOH= 4:1, λ_{ex} = 532 nm).

Table 1. I_D/I_G value for each sample in Raman spectroscopy.

Compounds	EG	WYK@EG	DFK@EG	DHK@EG
I _D /I _G	0.0952	0.3101	0.2729	0.2786

Carbon nanotubes (SWNT) and graphene (EG) have poor dispersibility, which greatly hinders their application [46]. Both Eugenii Katz [47] and Hans Jaegfeldt [48] have reported that the high aromatic system interacts strongly with the graphene surface through π -stacking. They confirmed the adhesion of the high aromatic system on the graphene surface by electrochemical measurement, and confirmed by controlled experiments that the irreversible adhesion of the high aromatic system on the graphene surface was formed by the non-covalent manner of the π -stacking of the aromatic ring. Both Hongjie Dai et al. [49] and Baek et al. [50] also found the similar strong interact on the surface of carbon nanotubes. Since the product has more benzene rings in the NDI and the branch, the benzene ring can interact with the carbon six-membered ring of the carbon material to attach the product to the EG (SWNT). As shown in **Figure 4**. If the

amphiphilic supramolecular we design can be bonded to the surface of the carbon material by π stacking through the fused aromatic structure of the NDI molecule, the polypeptide branch of the NDI molecule can improve the dispersion of the carbon material in solution. Since the combination of the fused aromatic ring structure and the carbon material is bonded by a non-covalent bond, the inherent structure of the carbon material is not changed. It is also possible to graft bioorganic molecules on the surface of the carbon material without destroying the intrinsic structure of the carbon material by attaching the bioorganic molecules to the amphiphilic supramolecular.

We ultrasonically complex the NDI product and EG in a mixed solution of chloroform and absolute ethanol (volume ratio 4:1) to obtain the NDI@EG product (Detailed experimental steps in the supporting information). We used Raman spectroscopy and TEM to verify that the NDI product was grafted onto the surface of the carbon material. The G peak at 1580 cm^{-1} in the graphene Raman spectrum is its main characteristic peak. The D peak is generally considered to be the disordered vibration peak of graphene. It is caused by lattice vibrations leaving the center of the Brillouin zone and is used to characterize structural defects or edges in graphene samples [51]. **Figure 5** is a Raman spectrum of graphene excited by a 532 nm laser. Since the graphene used in the experiment is a multilayer graphene (rather than a single-layer graphene) produced by the intercalation method in the laboratory, the graphene has more edges and contains partial defects. Obvious D peaks and weak D' peaks can be seen in the spectrum. However, the intensity of the D peak is not high, and the number of layers of the multilayer graphene can be roughly judged to be about 4 layers by the peak position of the G' peak and the relative height of the G peak and the G' peak [52]. In contrast, the D peak in the Raman spectrum of the composite product of NDI and graphene is much stronger, and the D' peak is also more pronounced. The

size of the I_D/I_G is usually used to indicate the degree of defect of the graphene. The I_D/I_G of each sample is shown in Table 1. It can be seen that the I_D/I_G values of the three samples are much larger than that of the pure EG, that is, the surface defects increase after the combination of graphene and NDI. The cause of surface defects is due to the adhesion of NDI molecules to the graphene surface through a carbon six-membered ring. **Figure 6** is the TEM images of pure EG and NDI@EG. It also can be seen from the electron microscopic image of EG that the graphene used in the experiment is a multilayer EG having a small number of layers, and is substantially transparent on the micro-gate by electron beam transmission. The black shadow in the image of NDI@EG is due to the fact that the transmitted electron beam does not pass through the film, but collides with atoms on the uneven surface to produce scattering. The pure carbon planar structure itself is almost completely transparent under TEM, and only when there are other substances or modifying groups, various kinds of shadows appear. This prove that NDI products do adhere to EG. The relevant images and data of the combination of NDI amphiphilic molecules and SWNT can be found in the **supporting information**.

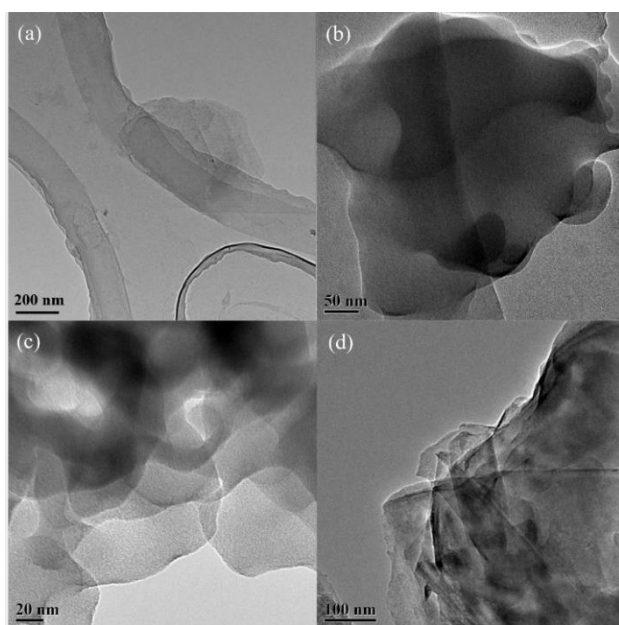


Figure 6. TEM images of (a) pure EG, (b) [WYK]₂-NDI @EG, (c) [DFK]₂-NDI @EG and (d)

[DHK]₂-NDI @EG distributed in CHCl₃: EtOH (4:1).

Fluorescence Imaging

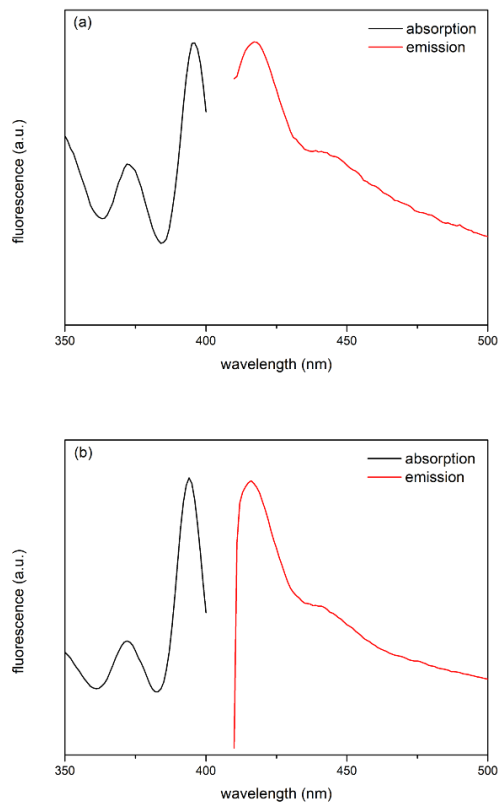


Figure 7. Fluorescence absorption (black line) and fluorescence emission (red line) spectra of (a) [DFK]₂-NDI and (b) [DHK]₂-NDI (0.05 wt% in acid solution).

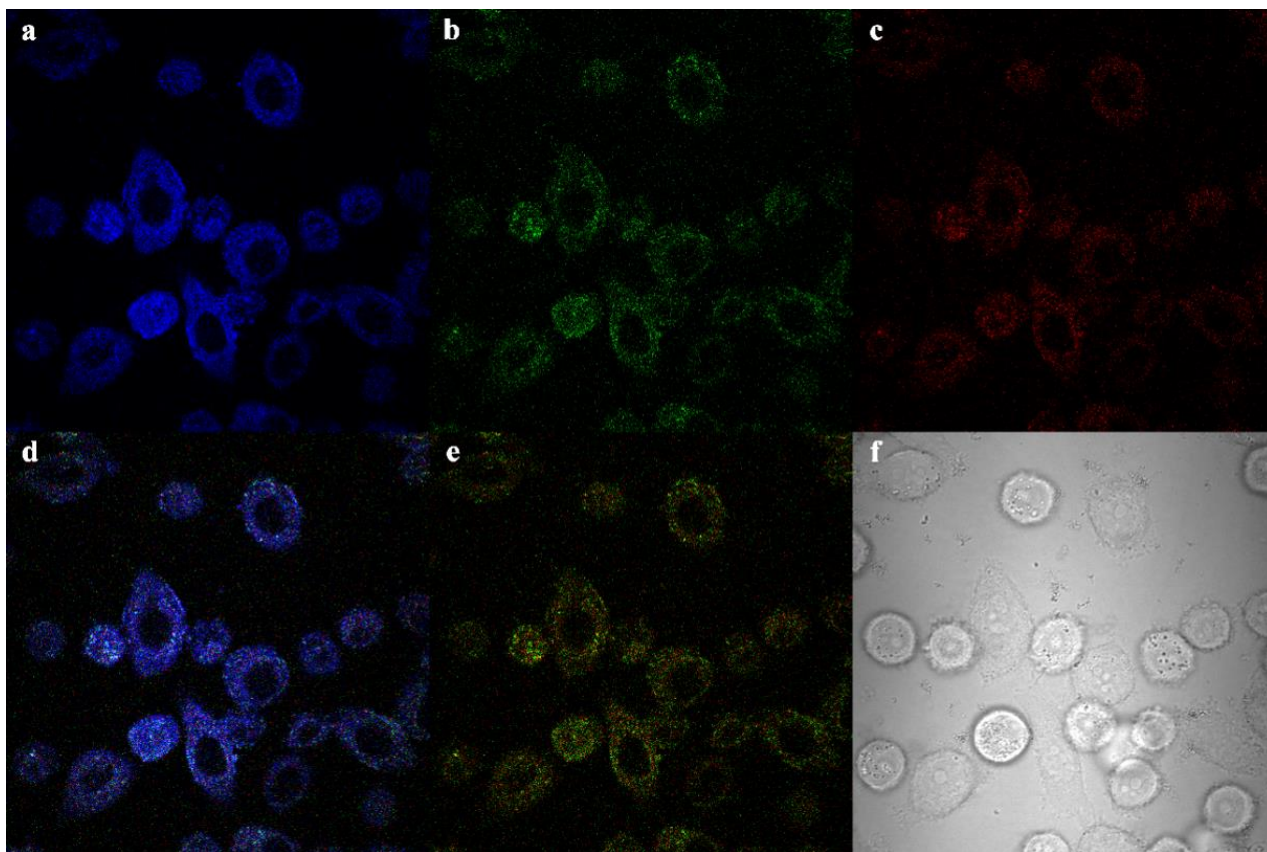


Figure 8. Single-photon laser-scanning confocal microscopy of PC-3 cells incubated for 20 min at 37 °C with [DFK]₂-NDI (10 mM in 1:99% DMSO: serum-free medium). (a) blue channel, (b) green channel, (c) red channel, (d)(e) mix channel, (f) DIC channel.

We have studied the fluorescence properties of NDI products. Fluorescence absorption spectroscopy results (**Figure 7**) show that the sample has a strong fluorescence absorption peak around 300 nm and 395 nm (detailed fluorescence spectra are in the **supporting information**). When the excitation wavelength is 395 nm, the fluorescence emission spectrum indicates that the sample has a clear emission peak in the visible light region. The intensity of the excitation light in the blue light wavelength range is particularly high. Therefore, we further studied the application of samples in fluorescence imaging.

We used PC-3 cells to study the fluorescence imaging of samples. EMEM medium (Eagle's

Modified Essential Medium) containing 15% fetal bovine serum (FCS), 200 U mL⁻¹ L-glutamine and 100 U mL⁻¹ penicillin was used in the experiment. Prior to imaging, 1 mL of fresh EMEM was added and the sample was added to give a final sample concentration of 10 mM (solution to DMSO). After culturing 20 molecules, a fluorescence image was observed using a confocal microscope.

There is no doubt that after the addition of the DMSO solution of the tripeptide-NDI molecule to the aqueous medium, the molecules will aggregate due to the hydrophobic action. T. Govindaraju [38] also reported that NDI polypeptide derivatives aggregate when the water (the highest polarity) is gradually added to the solution. However, it can be inferred that the size of the aggregates is not too large. PC-3 cells can absorb exogenous tripeptide-NDI molecular aggregates into the cytoplasm by endocytosis within 20 minutes. The final concentration of NDI molecules in the medium is less than 0.01 wt%, which is not conducive to molecular aggregation to form larger aggregates. At the same time, the final cell fluorescence imaging image also shows that the NDI molecules do absorb into the cytoplasm. The cell culture medium contains a large number of compounds necessary for the growth of cells such as amino acids, inorganic salts and alkaloids. The whole system is a very complex mixture system. Therefore, it is very complicated to research its aggregation in the medium. As can be seen from **Figure 8**, the tripeptide-NDI molecule showed clear fluorescence under the confocal microscope. In particular, the blue fluorescence is very noticeable, consistent with the results of the fluorescence excitation spectrum. Fluorescent images also indicate that the tripeptide-NDI molecule is absorbed by the cells and distributed in the cytoplasm. The cells showed good activity throughout the test. However, if it is used as a potential material for fluorescent probes, more research such as cytotoxicity is required.

Conclusion

Based on the aggregation tendency of tripeptides, we designed and synthesized three [tripeptide]₂-NDI amphiphilic supramolecular. NDI group as the self-assembling scaffold in NDI amphiphilic molecules provides additional π - π stacking for peptide self-assembly to further promote molecular aggregation. In the acidic or basic solution, the three molecules form different aggregate structures due to protonation effects and charge effects caused by pH changes. Under acidic condition, the nanosphere clusters ([WYK]₂-NDI) and the nano ([DFK]₂-NDI and [DHK]₂-NDI) were formed. Under basic condition, the needle-like clusters ([WYK]₂-NDI) or the micron-sized spheres ([DHK]₂-NDI), even the irregular aggregates ([DFK]₂-NDI) were formed. Both the UV absorption spectrum and the circular dichroism of the sample can reflect the degree of aggregation and regularity of the sample to some extent.

Since there are a plurality of benzene rings in the molecule, the NDI amphiphilic molecules can be effectively attached to the carbon six-membered ring of carbon nanotubes and graphene. The dispersibility of carbon nanotubes and graphene can be improved due to the presence of different groups of amino acid branches in the NDI molecule. It provides an idea for improving the dispersion of carbon nanotubes and graphene. Changing the type of polypeptide and using different amino acid branches can improve the dispersibility of carbon nanotubes and graphene in different solvents. A method of grafting bioorganic molecules on the surface of a carbon material without destroying the inherent structure of the carbon material is also provided. In addition, the fluorescent properties of its molecules make it a potential application in cell fluorescent probes.

In some aspects, the presently disclosed peptide-[organic electronic unit]-peptide structure has the property of self-assembly into a defined nanostructure under aqueous or physiological

condition. In certain aspects, the defined nanostructure has an electrical property, an optoelectronic property, and/or a cell imaging/adhesion property.

Supporting Information

Supporting information text: Organic synthesis details, characterization details, HPLC data and detailed H-NMR data could be found in the **supporting information**. There are also enlarged, clearly SEM self-assembled images for viewing. In addition, detailed fluorescence absorption and fluorescence emission spectra and more cell fluorescence imaging can be found. Detailed information on cell fluorescence preparation is also included.

Supporting Information File 1:

File Name: Supporting information

File Format: PDF

Title: Electronic Supporting Information

Acknowledgments

This study was supported financially by the National Natural Science Foundation of China (No. 21502226).

References

- (1) Ghadiri, M. R.; Granja, J. R.; Milligan, R. A.; McRee, D. E.; Khazanovich, N. *Nature* **1993**, *366* (6453), 324-327.
- (2) Zhang, S.; Holmes, T.; Lockshin, C; Rich, A. *Proc. Natl. Acad. Sci. U. S. A.* **1993**, *90*, 3334–3338.

-
- (3) Melchionna, M.; Styan, K. E.; Marchesan, S. *Curr. Top. Med. Chem.* **2016**, *16*, 2009-2018.
- (4) Sahab Negah, S.; Khaksar, Z.; Aligholi, H.; Mohammad Sadeghi, S.; Modarres Mousavi, S. M.; Kazemi, H.; Jahanbazi Jahan-Abad, A.; Gorji, A. *Mol. Neurobiol.* **2017**, *54*, 8050-8062.
- (5) Ouberai, M. M.; Santos, A. L. G. D.; Kinna, S.; Madalli, S.; Hornigold, D. C.; Baker, D.; Naylor, J.; Sheldrake, L.; Corkill, D. J.; Hood, J. *Nat. Commun.* **2017**, *8*, 1026.
- (6) Tagalakis, A. D.; Maeshima, R.; Yu-Wai-Man, C.; Meng, J.; Syed, F.; Wu, L. P.; Aldossary, A. M.; Mccarthy, D.; Moghimi, S. M.; Hart, S. L. *Acta Biomater.* **2017**, *51*, 351-362.
- (7) Hu, K.; Jiang, Y.; Xiong, W.; Li, H.; Zhang, P. Y.; Yin, F.; Zhang, Q.; Geng, H.; Jiang, F.; Li, Z. *Sci. Adv.* **2018**, *4*, eaar5907.
- (8) Zhang, S.; Marini, D. M.; Hwang, W.; Santoso, S. *Curr. Opin. Chem. Biol.* **2002**, *6* (6), 865-871.
- (9) Matson, J. B.; Zha, R. H.; Stupp, S. I. *Curr. Opin. Solid St. M.* **2011**, *15* (6), 225-235.
- (10) Qian, Y.; Wang, W.; Wang, Z.; Jia, X.; Han, Q.; Rostami, I.; Wang, Y.; Hu, Z. *ACS Appl. Mater. Inter.* **2018**, *10* (9), 7871-7881.
- (11) Katsuhiko Fujita; Shunsaku, Kimura, A.; Imanishi, Y. *Langmuir* **1999**, *15*, 4377-4379.
- (12) Shunsaku Kimura; Dohyung Kim; Junji, Sugiyama, A.; Imanishi, Y. *Langmuir* **1999**, *15*, 4461-4463.
- (13) Yanlian, Y.; Ulung, K.; Xiumei, W.; Horii, A.; Yokoi, H.; Shuguang, Z. *Nano Today* **2009**, *4* (2), 193-210.
- (14) Hamley, I. W. *Soft Matter* **2011**, *7* (9), 4122-4138.
- (15) FT, S.; NR, L.; X, G.; DM, R.; TM, D.; EA, A.; BL, N. *Mol. Biosyst.* **2011**, *7* (2), 486-496.
- (16) Liu, L.; Li, Q.; Zhang, S.; Wang, X.; Li, J.; Liu, Z.; Besenbacher, F.; Dong, M. *Adv. Sci.* **2016**, *3*, 1500369.

-
- (17) Marchesan, S.; Easton, C. D.; Styan, K. E.; Waddington, L. J.; Kushkaki, F.; Goodall, L.; Mclean, K. M.; Forsythe, J. S.; Hartley, P. G. *Nanoscale* **2014**, *6*, 5172-5180.
- (18) James, J.; Mandal, A. B. *J. Colloid Interf. Sci.* **2011**, *360*, 600-605.
- (19) Silvia, M.; Lynne, W.; Easton, C. D.; Winkler, D. A.; Liz, G.; John, F.; Hartley, P. G. *Nanoscale* **2012**, *4*, 6752-6760.
- (20) Silvia, M.; Easton, C. D.; Firdawosia, K.; Lynne, W.; Hartley, P. G. *Chem. Commun.* **2012**, *48*, 2195-2197.
- (21) PW, F.; GG, S.; YM, A.; D, K.; CG, P.; N, J.; NT, H.; RV, U.; T, T. *Nat. Chem.* **2015**, *7* (1), 30-37.
- (22) Elsayy, M.; Smith, A. M.; Hodson, N.; Squires, A. M.; Miller, A. F.; Saiani, A. *Langmuir* **2016**, *32* (19), 4917-4923.
- (23) Liu, Y. H.; Hsu, S. M.; Wu, F. Y.; Cheng, H.; Yeh, M. Y.; Lin, H. C. *Bioconjugate Chem.* **2014**, *25* (10), 1794-1800.
- (24) Rajdev, P.; Molla, M. R.; Ghosh, S. *Langmuir* **2014**, *30* (8), 1969-1976.
- (25) Chen, Z.; Lohr, A.; Saha-Moeller, C. R.; Wuerthner, F. *Chem. Soc. Rev.* **2009**, *38* (2), 564-584.
- (26) Jana, P.; Bera, S.; Paikar, A.; Haldar, D. *Cryst. Growth Des.* **2014**, *14* (8), 3918-3922.
- (27) S, F.; RV, U. *Chem. Soc. Rev.* **2014**, *43* (23), 8150-8177.
- (28) Debnath, S.; Shome, A.; Das, D.; Das, P. K. *J. Phys. Chem. B* **2010**, *114* (13), 4407-4415.
- (29) Fatás, P.; Bachl, J.; Oehm, S.; Jiménez, A. I.; Cativiela, C.; Díaz, D. D. *Chem. Eur. J.* **2013**, *19* (27), 8861-8874.
- (30) Lei, L.; Yibao, L.; Dan, X.; Christian, B.; Shuai, Z.; Yanlian, Y.; Pedersen, J. S.; Chen, W.; Flemming, B.; Mingdong, D. *Nanoscale*, **2015**, *7*, 2250–2254.

-
- (31) Fleming, S.; Debnath, S.; Frederix, P. W. J. M.; Hunt, N. T.; Ulijn, R. V. *Biomacromolecules* **2014**, *15* (4), 1171-1184.
- (32) Bartocci, S.; Berrocal, J. A.; Guarracino, P.; Grillaud, M.; Franco, L.; Mba, M. *Chem. Eur. J.* **2017**, *24*, 2920-2928.
- (33) Bhosale, S. V.; Jani, C. H.; Langford, S. J. *Chem. Soc. Rev.* **2008**, *37*, 331-342.
- (34) Jones, B. A.; Facchetti, A.; And, M. R. W.; Marks, T. J. *J. Am. Chem. Soc.* **2007**, *129* (49), 15259-15278.
- (35) Katz, H. E.; Jerainne Johnson; And, A. J. L.; Li, W. *J. Am. Chem. Soc.* **2000**, *122* (32), 7787-7792.
- (36) Asir, S.; Demir, A. S.; Icil, H. *Dyes Pigments* **2010**, *84* (1), 1-13.
- (37) Mpima, S.; Ohnmacht, S. A.; Barletta, M.; Husby, J.; Pett, L. C.; Gunaratnam, M.; Hilton, S. T.; Neidle, S. *Bioorgan. Med. Chem.* **2013**, *21* (20), 6162-6170.
- (38) Avinash, M. B.; Govindaraju, T. *Nanoscale* **2011**, *3* (6), 2536-2543.
- (39) Bhosale, S. V.; Jani, C.; Lalander, C. H.; Langford, S. J. *Chem. Commun.* **2010**, *46* (6), 973-975.
- (40) Rao, K. V.; George, S. J. *Org. Lett.* **2010**, *12* (11), 2656-2659.
- (41) Chang, S.; Wu, X.; Li, Y.; Niu, D.; Gao, Y.; Ma, Z.; Gu, J.; Zhao, W.; Zhu, W.; Tian, H. *Biomaterials* **2013**, *34* (38), 10182-10190.
- (42) Frank, W.; Kaiser, T. E.; Saha-Moller, C. R. *Angew. Chem. Int. Ed.* **2011**, *50*, 3376-3410.
- (43) Xiang, J.; Yang, X.; Chen, C.; Tang, Y.; Yan, W.; Xu, G. *J. Colloid Interf. Sci.* **2003**, *258* (1), 198-205.
- (44) Bortolini, C.; Klausen, L. H.; Hoffmann, S. V.; Jones, N. C.; Saadeh, D.; Wang, Z.; Knowles, T.; Dong, M. *ACS Nano* **2018**, *12*, 5408-5416.

-
- (45) Bortolini, C.; Liu, L.; Hoffmann, S. V.; Jones, N. C.; Knowles, T. P. J.; Dong, M. *ChemistrySelect* **2017**, *2*, 2476-2479.
- (46) Chao, Z.; Shu, H.; Weng, W. T.; Wei, F.; Liu, T. *J. Mater. Chem.* **2012**, *22* (6), 2427-2434.
- (47) Katz, E. *Chem.* **1994**, *365*, 157-164.
- (48) Jaegfeldt, H.; Kuwana, T.; Johansson, G. *J. Am. Chem. Soc.* **1983**, *105*, 1805-1814.
- (49) Chen, R. J.; Zhang, Y.; Wang, D.; Dai, H. *J. Am. Chem. Soc.* **2001**, *123*, 3838-3839.
- (50) Baek, Y. K.; Jung, D. H.; Yoo, S. M.; Shin, S.; Kim, J. H.; Jeon, H. J.; Choi, Y. K.; Lee, S. Y.; Jung, H. T. *J. Nanosci. Nanotechnol.* **2011**, *11*, 4210-4216.
- (51) Popov, V. N.; Henrard, L.; Lambin, P. *Carbon* **2009**, *47* (10), 2448-2455.
- (52) Ferrari, A. C.; Meyer, J. C.; Scardaci, V.; Casiraghi, C.; Lazzeri, M.; Mauri, F.; Piscanec, S.; Jiang, D.; Novoselov, K. S.; Roth, S.; Geim, A. K. *Phys. Rev. Lett.* **2006**, *97*, 187401.

